THE JOURNAL OF BIOLOGICAL CHEMISTRY VOL. 287, NO. 21, pp. 17882–17893, May 18, 2012

Sequence Variation in Promoter of *Ica1* Gene, Which Encodes Protein Implicated in Type 1 Diabetes, Causes Transcription Factor Autoimmune Regulator (AIRE) to Increase Its Binding and Down-regulate Expression*[S]

Received for publication, November 3, 2011, and in revised form, March 15, 2012 Published, JBC Papers in Press, March 24, 2012, DOI 10.1074/jbc.M111.319020

Samantha M. Bonner[‡1], Susan L. Pietropaolo[‡1], Yong Fan[§], Yigang Chang[‡], Praveen Sethupathy[¶], Michael P. Morran[‡], Megan Beems[‡], Nick Giannoukakis[§‖], Giuliana Trucco[‖], Michael O. Palumbo[**], Michele Solimena[‡‡], Alberto Pugliese[§§], Constantin Polychronakos[**], Massimo Trucco[§], and Massimo Pietropaolo[‡2]

From the [‡]Laboratory of Immunogenetics, Brehm Center for Diabetes Research, Department of Internal Medicine, University of Michigan Medical School, Ann Arbor, Michigan 48105, the [§]Division of Immunogenetics, Department of Pediatrics, Rangos Research Center, University of Pittsburgh School of Medicine, Pittsburgh, Pennsylvania 15224, the [¶]Department of Genetics, University of North Carolina, Chapel Hill, North Carolina 27599, the [‖]Department of Pathology, University of Pittsburgh School of Medicine, Pittsburgh, Pennsylvania 15213, the [**]Endocrine Genetics Laboratory, Montreal Children Hospital-Research Institute, McGill University Health Center, Montreal, Quebec H3H 1P3, Canada, the [‡‡]Department of Molecular Diabetology, Paul Langerhans Institute Dresden, Carl Gustav Carus School of Medicine, Dresden University of Technology, 01307 Dresden, Germany, and the [§§]Immunogenetics Program, Diabetes Research Institute, Department of Medicine, Division of Endocrinology, Diabetes and Metabolism, Miller School of Medicine, University of Miami, Miami, Florida 33136

Background: Immunologic tolerance to tissue-restricted self-antigens primarily takes place in the thymus.
Results: Sequence variation within the *Ica1* promoter is associated with increased autoimmune regulator (AIRE) binding and transcription repression of ICA69 in medullary thymic epithelial cells.
Conclusion: AIRE is a transcription repressor within the NOD mouse *Ica1* promoter.
Significance: A newly identified role for AIRE as a transcription repressor in medullary thymic epithelial cells.

ICA69 (islet cell autoantigen 69 kDa) is a protein implicated in type 1 diabetes mellitus in both the non-obese diabetic (NOD) mouse model and humans. ICA69 is encoded by the *Ica1* gene on mouse chromosome 6 A1-A2. We previously reported reduced ICA69 expression in the thymus of NOD mice compared with thymus of several non-diabetic mouse strains. We propose that reduced thymic ICA69 expression could result from variations in transcriptional regulation of the gene and that polymorphisms within the *Ica1* core promoter may partially determine this transcriptional variability. We characterized the functional promoter of *Ica1* in NOD mice and compared it with the corresponding portions of *Ica1* in non-diabetic C57BL/6 mice. Luciferase reporter constructs demonstrated that the NOD *Ica1* promoter region exhibited markedly reduced luciferase expression in transiently transfected medullary thymus epithelial (mTEC$^+$) and B-cell (M12)-derived cell lines. However, in a non-diabetic strain, C57BL/6, the *Ica1* promoter region was transcriptionally active when transiently transfected into the same cell lines. We concomitantly identified five single nucleotide polymorphisms within the NOD *Ica1* promoter. One of these single nucleotide polymorphisms increases the binding affinity for the transcription factor AIRE (autoimmune regulator), which is highly expressed in thymic epithelial cells, where it is known to play a key role regulating self-antigen expression. We conclude that polymorphisms within the NOD *Ica1* core promoter may determine AIRE-mediated down-regulation of ICA69 expression in medullary thymic epithelial cells, thus providing a novel mechanistic explanation for the loss of immunologic tolerance to this self-antigen in autoimmunity.

Accumulating evidence indicates that organ-specific molecules are naturally expressed in the thymus and peripheral lymphoid organs (1, 2). Tolerance to tissue-restricted self-molecules is believed to begin in the thymus during maturation of the immune system with the deletion of thymocytes exhibiting strong affinity T-cell receptors towards self-molecules (3–5). The insulin gene is one of the most widely studied genes in both humans and mice, exhibiting thymic expression as well as a β-cell expression-dependent association with T1D[3] susceptibility (2, 6–9). For instance, in humans, the *IDDM2* suscepti-

* This work was supported, in whole or in part, by National Institutes of Health (NIH) Grants R01 DK53456 and R01 DK56200; NIH, NIDDK, Grant PA-04-081 (to M. P.); NIH Grant R01 DK24021 (to M. T.); NIH Grant R01 AI-44456 (to A. P.); and NIH Grants DK-53015 and 54913 (to M. S.). This work was also supported by Juvenile Diabetes Research Foundation Grant 4-1999-945 (to M. T.), an American Diabetes Association Career Development Award (to M. P.), and Juvenile Diabetes Research Foundation Career Development Award 296117 (to A. P.). This work was also partially supported by grants from the German Center for Diabetes Research, the German Federal Ministry for Education and Research, and the Alexander Von Humboldt Foundation (to M. S.).
[S] This article contains supplemental Table 1.
[1] These authors contributed equally to this work.
[2] To whom correspondence should be addressed: Laboratory of Immunogenetics, Brehm Center for Diabetes Research, University of Michigan Medical School, 1000 Wall St., Ann Arbor, MI 48105. E-mail: maxtp@umich.edu.

[3] The abbreviations used are: T1D, type 1 diabetes mellitus; VNTR, variable number of tandem repeat(s); NOD, non-obese diabetic; SNP, single nucleotide polymorphism; RMA, robust multiple-array averaging; PWM, positional weight matrix; TF, transcription factor.

bility locus of the insulin gene (*INS*) is a region associated with T1D and has been finely mapped to reveal variable number of tandem repeat (VNTR) polymorphisms upstream of the *INS* promoter. The length of these repeats has been directly implicated in the control of the expression levels of insulin mRNA in the thymus (9–11). In addition to insulin, ICA69 (islet cell autoantigen 69 kDa), a neuroendocrine protein targeted by autoimmmune responses in human T1D and in non-obese diabetic (NOD) mice (12–14), is also expressed in the thymus, and we considered the likelihood that thymic levels of ICA69 would affect susceptibility to T1D through a mechanism similar to that shown for the insulin VNTRs (2, 15). This hypothesis is primarily based on our previous studies indicating that IA-2, GAD65, and ICA69 are transcribed in the human thymus throughout fetal life and childhood (2, 10, 16). The significance of thymic ICA69 expression in T1D susceptibility was reinforced through experiments involving tetracycline-responsive transgene promoter studies in the NOD mouse model, which exogenously overexpressed ICA69 in the thymus and spleen (14). This overexpression of thymic ICA69 resulted in a significant delay of disease progression in this model (14).

Given that thymic ICA69 expression is significantly reduced in NOD mice compared with other non-diabetic mouse strains (15), we now posit the existence of DNA sequence variation with the potential for functionally relevant effects on *Ica1* gene expression in the thymus. Such variations in the *Ica1* promoter might lead to an increased probability of failure to negatively select ICA69-reactive T-cell clones of developing thymocytes. Therefore, sequence variations in the *Ica1* promoter may potentially affect tissue-restricted genes functionally involved in autoimmunity and T1D. In the present study, we 1) establish sequence variation in the *Ica1* promoter of NOD and non-diabetic mice, 2) associate the variations with deficient expression of ICA69 in a cell-based model, and 3) provide evidence for a novel functional interaction of AIRE binding with *Ica1* transcriptional regulation.

EXPERIMENTAL PROCEDURES

Cell Lines—Medullary thymic epithelial cell line (mTEC$^+$) positive for insulin production was kindly provided by Dr. Constantin Polychronakos (Endocrine Genetics Laboratory, Montreal Children's Hospital) and grown using complete Minimum Essential Medium Eagle's (MEM) following previously published protocols (7). The mouse B-cell line (M12), generously provided by Dr. Wesley Dunnick (University of Michigan, Ann Arbor, MI), was propagated in RPMI 1640 complete medium following previously published protocols (17).

Generation and Subcloning of Constructs—We have previously characterized the human *ICA1* promoter region (18). Based on our previous findings and DNA sequence similarity with human *ICA1*, specific primers were designed for the putative mouse *Ica1* promoter element as follows: 5′ primer, GAATTCTTATATTTTCATGTAATT; 3′ primer, GAGTGTGAATTTCATAATCGTG. Due to the GC-rich nature of the *Ica1* promoter region, DNA samples were amplified for 35 cycles using the LA Taq™ PCR kit (Takara Mirus Bio, Madison, WI) and corresponding buffers. Amplified PCR products from NOD and C57BL/6 genomic DNA were directly subcloned into the pCR®II-TOPO vector (Original TA Cloning Kit, Invitrogen) following the manufacturer's protocol. Cloning of *Ica1* promoter elements was performed using the pGL3-Basic vector as described previously and later used in the luciferase assays (18). The pGL3 vectors containing the *Ica1* promoter elements were sequence-verified utilizing a series of overlapping primer sets at the University of Michigan Sequencing Core.

Luciferase Assays—Both mTEC$^+$ and M12 cell lines were assessed for luciferase reporter activity using the Dual-Luciferase reporter assay (Promega, Madison, WI). The protocol was followed as described by the manufacturer for both cell lines with the exception of a 30-min shaking incubation for the passive lysis step. Transfections were prepared as described below for each respective cell line, and the luciferase assays were read using the BD Monolight 3010 luminometer.

The mTEC$^+$ cells were grown in 12-well plates in complete MEM at a density of 0.9×10^5 cells/well 18 h prior to transient transfection to ensure 70–80% confluence at the time of transfection. The mTEC$^+$ cells were transfected in triplicate with the Luciferase pGL3-*Ica1* constructs and the proper positive and negative control vectors using the Fugene HD transfection reagent (Roche Applied Science) at a ratio of 8:2 (8 μl of reagent, 2 μg of DNA).

M12 cells were plated in 24-well plates in complete RPMI 1640 medium at a density of 5.0×10^5 cells/well 18 h prior to transfection. Luciferase pGL3-*Ica1* constructs and the proper positive and negative control vectors were transfected using Effectene transcription reagent (Qiagen Inc., Valencia, CA) at a ratio of 1:20 (DNA/Effectene).

The respective transfection reagent to pGL-3 *Ica1* DNA construct ratio was held constant for each tested construct for that cell line described above. To allow for normalization of firefly luciferase values based on transfection efficiency, the co-reporter vector pRL-TK expressing *Renilla* luciferase was included in the transfection mixture at a ratio of 1:10 (co-reporter plasmid/experimental promoter construct) as reported previously (18).

Mutagenesis—The pGL3-Basic vector containing the C57BL/6 *Ica1* sequence was used as the backbone to generate three separate constructs by inserting different combinations of multiple SNPs from the NOD *Ica1* promoter sequence referred to as Construct 1, Construct 2, and Construct 3. Construction began with sequential digests of both the C57BL/6 and NOD *Ica1* sequences with restriction enzymes at 37 and 55 °C, respectively. This was done to create a gap in the C57BL/6 *Ica1* sequence into which a corresponding NOD *Ica1* fragment sequence containing specific SNPs would be inserted. Construct 1 required the use of ZraI and BsmBI, such that the NOD 125-base pair fragment containing SNPs (−)70 and (−)117 were ligated into the C57BL/6 sequence between base pairs 1381 and 1506. Construct 2 required the use of SexAI and BsmBI, such that the NOD 358-base pair fragment containing SNPs at (−)304, (−)190, (−)117, and (−)70 were ligated into the C57BL/6 sequence between base pairs 1144 and 1506. Construct 3 required the use of enzymes Pm1I and BsmBI, such that the NOD 506-base pair fragment containing SNPs (−)471, (−)304, (−)190, (−)117, and (−)70 were ligated into the

C57BL/6 sequence between base pairs 1000 and 1506. One Shot® Top 10 competent cells (Invitrogen) were transformed to generate pure plasmid DNA preparations for use in the luciferase assays. All constructs were sequence-verified to contain the appropriate SNPs utilizing overlapping primer sets at the University of Michigan Sequencing Core.

Isolation of mTEC$^+$ Cells and Microarray Expression Profiling—Isolation of thymic antigen presenting stromal cells was performed as described previously (8). Briefly, thymi harvested from seven 5–6-week-old C57BL6/129 mice were needle-dissected into small pieces, collagenase-digested into single cells, and negatively selected with anti-CD90 antibody-conjugated magnetic microbeads to deplete thymocytes (Miltyeni, Auburn, CA). The stromal cells were separated further with an anti-CD45 microbead kit, followed by FACS into CD45$^+$, MHC II$^+$, CD11c$^-$ macrophages and B-cells; CD45$^+$, MHC II$^+$, CD11c$^+$ thymic dendritic cells; CD45$^-$, EpCAM$^+$, UEA-1^{high}, Ly51^{low} medullary thymic epithelial cells (mTECs); and CD45$^-$, EpCAM$^+$, UEA-1^{low}, Ly51^{high} cortical thymic epithelial cells.

Total RNA was isolated with the RNeasy microkit (Qiagen, Valencia, CA), following the manufacturer's procedures, and reverse transcribed with the Superscript III cDNA synthesis kit (Invitrogen). The following primers and conditions were used to examine gene expression: *Ica1*, 5′-TGAGTCTGCAACCTTCAACAGGGA-3′ and 5′-AAACAGGGCCTTGACCCTCTCATT-3′, 40 cycles with LA *Taq* polymerase (Takara Mirus Bio, Madison, WI); cytokeratin 2/8 (K2-8), 5′-AGGAGCTCATTCCGTAGCTG-3′ and 5′-TCTGGGATGCAGAACATGAG-3′, 35 cycles with Titanium *Taq* (Clontech); Hprt, 5′-GCGTCGTGATTAGCGATGATGAAC-3′ and 5′-CCTCCCATCTCCTTCATGACATCT-3′, 35 cycles with Titanium *Taq* (Clontech, Mountain View, CA).

Insulin-expressing mTEC$^+$ cells were isolated and grown as described (37). Briefly, the cells were passaged at 33 °C and grown in triplicate in 10-cm tissue culture dishes to 80–90% confluence. RNA was extracted using the RNeasy minikit (Qiagen, Mississauga, Canada) and treated with Ambion DNase I (Ambion, Austin, TX), and 10 μg from each of the triplicate samples was applied to the Affymetrix (Santa Clara, CA) Mouse Genome 430 2.0 arrays (containing 45,102 probe sets representing 39,000 transcripts).

Prior to microarray analysis, RNA quality was verified using electrophoretic detection of the 18S and 28S peaks in an Agilent 2100 Bioanalyzer (Agilent, Colorado Springs, CO). Microarray data were normalized using robust multiple-array averaging (RMA), as log2 values. To determine the expression of a given gene, relative to the rest of the transcriptome, its value was placed on a frequency histogram of expression levels relative to the rest of the genes on the array.

Identification of Transcription Factor Binding Sites—Transcription factor binding site prediction was performed by implementing the previously described PWM-Scan algorithm (19). First, we mined the Transfac database (release 2010.1 from Biobase) for 1,302 positional weight matrices (PWMs), each of which corresponds to a transcription factor (TF) binding motif. We then searched for high affinity matches (p value of <0.0001) to these PWMs in the NOD mouse *Ica1* promoter region. This p value threshold corresponds to an average expected frequency of 1 match every 10 kb. We considered the identified PWM matches as putative transcription factor binding sites. We implemented this algorithm for both alleles at three mutated loci positions: (−)471 C/A; (−)117 G/A; (−70) G/A, where the mutations correspond to the alleles in the wild type genetic background of C57BL/6 mice (supplemental Table 1). At each mutant locus, we identified two classes of transcription factor binding sites: 1) those that are predicted only with one allele and 2) those that are predicted with both alleles but have substantially different PWM affinity scores.

TABLE 1
Biotinylated and unlabeled capture probes used to detect AIRE transcription factor binding activity using the NoShift transcription factor assay
The SNP is shown in capitalized boldface type at the putative recognition site.

Oligonucleotides	Sequence (5′–3′)
NOD (−)471 sense[a]	Biotin-agataccctaga**A**atgggggtcacg
NOD (−)471 antisense[a]	Biotin-cgtgacccccat**T**ctagggtatct
NOD (−)471 sense	agataccctaga**A**atgggggtcacg
NOD (−)471 antisense	cgtgacccccat**T**ctagggtatct
C57BL/6 sense	agataccctaga**C**atgggggtcacg
C57BL/6 antisense	cgtgacccccat**G**ctagggtatct

[a] Biotinylated oligonucleotide.

AIRE Binding Assay—Nuclear fractions of mTEC$^+$ and M12 cells were prepared using the NE-PER nuclear and cytoplasmic extraction kit and protocol (Pierce). The binding of AIRE in nuclear extracts to the targeted sequence located at SNP (−)471 was determined using the NoShift® transcription factor assay kit and the corresponding protocol (Novagen Inc., Gibbstown, NJ). The oligonucleotide sequences are listed in Table 1.

The specificity of AIRE TF binding to the NOD (−)471 site was determined utilizing a previously reported methodology (20) and the NoShift® protocol with the following exception. The non-biotinylated competitor oligonucleotides for NOD (−)471 and the C57BL/6 were used at 200 pmol per reaction, a 20:1 excess compared with the biotinylated NOD (−)471. This ratio is well within the range suggested in the NoShift® protocol for a 20-μl reaction. The primary antibody was anti-mouse AIRE (eBioscience, San Diego, CA) diluted 1:50, and the secondary antibody was horseradish peroxidase (HRP)-conjugated anti-rat IgG (Abcam, Cambridge, MA) diluted 1:1000. The assays were performed in triplicate, and absorbance was measured using a PerkinElmer Life Sciences Victor^{3}V 1420 multilabel plate reader.

Isolation of CD45$^-$ Stromal Cells from Lymph Nodes—Lymph nodes (pancreatic, mesenteric, and axillary) were harvested from 3–4 NOD, C57BL/6, and B6.129S2-*Aire*$^{tm1.1Doi}$/J (6–8 weeks old; Jackson Laboratory, Bar Harbor, ME) and digested with collagenase. In this mouse, exon 2 and portions of the flanking introns of the *Aire* gene were deleted by Cre-lox-mediated homologous recombination. Analysis of the mutated *Aire* transcript identified a frameshift that precludes translation past exon 1. The separated single cells were negatively selected with anti-CD45 antibody-conjugated magnetic beads (Miltenyi, Auburn, CA), followed by positive selection with anti-MHC II microbeads for MHC II+, CD45$^-$ stromal cells. RT-PCR was performed according to previously published methods (8).

Tissue Samples—Tissues from adult autopsy cases (spleen, lymph nodes, and thymus) were provided by the Cell Trans-

plant Center, Diabetes Research Institute at the University of Miami (21) and from the Department of Pathology of the University of Pittsburgh. From the available cases, 13 thymus, 25 spleen, and 3 lymph node specimens and 4 thymus, 2 spleen, and 1 lymph node specimens were used for ICA69 staining. The following tissues are from subjects who were not known to have T1D: thymus 1892: 2 days old, African American male; thymus 1897: 36 weeks old, Caucasian male; spleen and lymph node 2040, 40 weeks old, African American female; thymus and spleen 2892: 24 weeks old, African American female; and thymus 3222: 21 weeks old, African American female. All tissues collected were obtained through the proper ethical and administrative procedures of both institutions.

Immunohistochemistry—Human thymus tissue sections (6 μm) were fixed in paraformaldehyde (4% in phosphate-buffered saline, pH 7.4) and then paraffin-embedded according to previously published protocols (15, 21). Human spleen and lymph node frozen sections (5 μm) were fixed in 2% buffered formalin. Mouse anti-human ICA69 antibody was generated in our laboratory from the hybridoma, IA-A564. The primary antibody was used at a dilution of 1:50 for both paraffin-embedded and frozen tissues. Negative controls included omission of the primary antibody and incubation with an isotype control antibody as primary antibody. Human thymus tissues were stained using the LSAB kit (Dako, Carpinteria, CA) according to the manufacturer's protocol with the addition of a mild permeabilization method prior to the application of the primary antibody (22). Slides were then counterstained with Gill's hematoxylin solution. Human spleen and lymph node preparations were stained using the streptavidin-biotin-peroxidase method and aminoethylcarbazole (*red*) as substrate for the horseradish peroxidase enzyme (Zymed Laboratories Inc., San Francisco, CA).

Isolation of RNA and Detection of ICA69 in Mouse Thymic Tissue—Thymus tissue was harvested from three 5-week-old female C57BL/6 and NOD mice and homogenized in TRIzol® according to the manufacturer's protocol (Invitrogen) to generate total RNA. We used standard cDNA two-step processing using the Maloney murine leukemia virus reverse transcriptase (Epicenter, Madison, WI) according to the manufacturer's protocol. The cDNA was then generated from total RNA for each strain to be used for PCR analysis.

The PCRs each contained 5 μl of cDNA, 1 μl of LA *Taq* (Takara Mirus Bio, Madison, WI), including primers in a total reaction volume of 50 μl. Thirty cycles were completed at 94 °C, denaturation for 30 s, 58 °C annealing for 30 s, and 72 °C elongation for 45 s. Primers used were mICA69Fr (CACCATGTCAGGACACAAATGTTATTCCTGGGAG) and mICA69Rv (GTTCACTGTCAGCCAGGTATCAGAGATGGC). Amplification using a primer set specific for glyceraldehyde-3-phosphate dehydrogenase (GAPDH) was carried out to test the integrity of the cDNA using the Mouse GAPDH Primer Set Kit (Maxim Biotech, Inc. Rockville, MD) (data not shown). The ICA69-generated PCR fragment was gel-purified, and the nucleotide sequence was verified using overlapping primer sets at the University of Michigan Sequencing Core.

Statistical Analysis—Results were reported as the mean ± S.E. of replicates described throughout. Luciferase assay and AIRE binding assay values between groups were compared using the Mann-Whitney test. p values less than 0.05 were considered significant.

RESULTS

Expression of ICA69 in Human Thymus and Peripheral Lymphoid Organs—We have previously reported that ICA69 transcripts were detected by RT-PCR in human thymi at different stages of maturation (both fetal and postnatal tissues) (2). We now show that an ICA69 mAb can detect the protein expressed in human thymus tissue sections (Fig. 1). Fig. 1*A* illustrates the presence of ICA69-positive stained cells found predominantly within the thymic medulla region of human thymus paraffin sections. The antibody specific staining of these cells, as shown in Fig. 1*B*, disappears after the ICA69 mAb is absorbed with the recombinant ICA69 protein prior to the staining procedure. Additionally, there was no staining when a control isotype antibody was used with or without the secondary antibody (data not shown). ICA69-positive cells were also detected in human spleen and lymph node frozen sections shown in Fig. 1, *C* and *D*, respectively. The proportion of cells that stained positive for ICA69 ranged from 1 to 3% in most evaluated sections.

Ica1 Is Predominantly Expressed in mTEC within Thymus—Our previous studies with both human and mouse tissues (2, 15) were further expanded through FACS of thymocytes and microarray expression profile examination, whether or not there was significant expression of ICA69 in insulin-expressing medullary thymic epithelial cells. Mouse thymi from C57Bl6/129 mice were harvested, digested with collagenase, and separated into four stromal populations via magnetic beads and FACS, as described previously (8). The cell population $CD45^{-}$, $EpCAM^{+}$, UEA-1^{high}, and $Ly51^{low}$ (mTECs) in Fig. 2*A*, *lane R3*, shows evidence that *Ica1* expression is found predominantly in the medullary thymic epithelial cells. It is well known that this same subpopulation of medullary thymic epithelial cells ($CD45^{-}$, $EpCAM^{+}$, UEA-1^{high}, $Ly51^{low}$) express AIRE in addition to a specific pattern of costimulatory molecules, including CD40, CD80, and PD-L1 (23, 24). The results, shown in Fig. 2*B*, indicate a biologically significant expression of *Ica1* in the microarray profiling of an insulin-expressing medullary thymic epithelial ($mTEC^{+}$) cell line. To determine the expression of a given gene, relative to the rest of the transcriptome, its value was placed on a frequency histogram in relation to the expression levels of other genes in the array. *Ica1* gene expression is found to be within the 64th percentile relative to the expression of the rest of the transcriptome.

Characterization of Ica1 Core Promoter Elements—We identified the 5′-flanking region of the mouse *Ica1* gene (GenBank™ accession number JF513202) by initially examining the degree of homology between the human *ICA1* promoter (18) and the corresponding mouse nucleic acid sequences available in the NCBI GenBank™ data base. Homology searches of nucleic acid sequences revealed an ~85% identity between the human and the putative mouse promoter core sequence of the *Ica1* gene, which maps on chromosome 6 A1-A2. Based on this high degree of nucleotide sequence similarity, we designed specific oligonucleotides and amplified a 2.6-kb genomic DNA PCR product from both NOD and C57BL/6 mouse strains. The

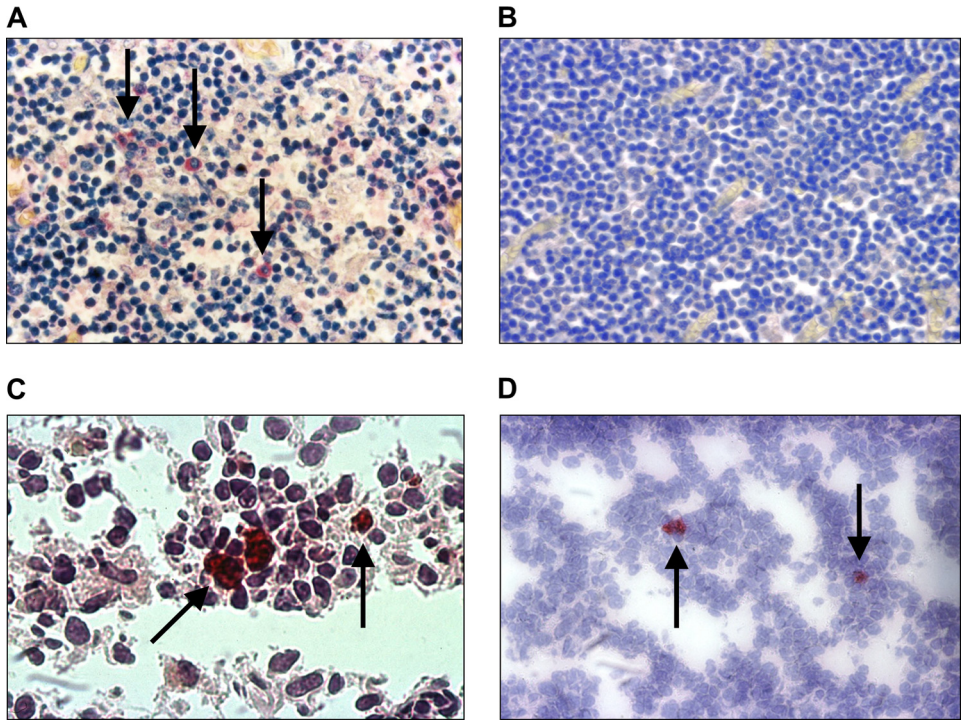

FIGURE 1. **ICA69 autoantigen expression in the human thymus (*A* and *B*), spleen (*C*), and lymph node (*D*) denoted with *arrows*.** *A*, a microphotograph of ICA69 using the ICA69 mAb and alkaline phosphatase immunoenzymatic detection. Staining of a paraformaldehyde-fixed section of human thymus with the ICA69 mAb shows selective staining for a cell subtype that is present predominantly in the medulla (×200). *B*, ICA69-specific staining disappears after absorbing out the ICA69 mAb with the recombinant human ICA69 molecule against which this mAb was produced (×200). *C* and *D*, immunostaining of spleen (×400) and lymph node (×200) frozen sections after incubation with the ICA69 mAb detected with the streptavidin-biotin-peroxidase method and the aminoethylcarbazole substrate (*red*) and counterstaining with hematoxylin.

resulting gel-purified or undiluted PCR products were subsequently subcloned into the pCR®II-TOPO vector (18) and sequenced. Given the high degree of similarity with the human *ICA1* promoter (18), we have termed the *Ica1* 5′-UTR exon sequences exons A, B, and C rather than adopt the −3, −2, −1 exon notation proposed by Gaedigk *et al.* (25). We have adopted this notation to maintain consistency with our previous studies of the human *ICA1* promoter (18) and for ease in recognition of the sequence similarity of the mouse *Ica1* promoter. The *Ica1* promoter sequence is summarized as an illustration in Figs. 3 and 4.

We then began to consider putative functional characteristics of the *Ica1* 5′-regulatory elements. Similar to the *ICA1* promoter (18), initiation of *Ica1* transcription was found to originate from any one of three distinct 5′-untranslated exons with independent transcription initiation signals characteristic of non-TATA, non-CCAAT, or GC-rich promoters. Remarkably, we found that almost all potential transcription activator sequences and TF binding sites were identical to those found in the human *ICA1* promoter (Figs. 3 and 4). Surrounding the putative transcription initiation site(s) are motifs characteristic of consensus Sp1/Sp3/GC-boxes and cAMP-responsive element-binding protein sites. In order to determine if these differences in transcriptional activity were due to cis-acting variations, we aligned the two 2.6-kb genomic DNA sequences from NOD and C57BL/6 mice and found that the NOD mouse *Ica1* promoter exhibited five unique nucleotide differences, SNPs, compared with the C57BL/6 *Ica1* promoter. These nucleotide differences are specific to the NOD strain and are not found in the other non-diabetes disease-prone mouse strains examined, including C57BL/6, Balb/c, and SWR. The five SNPs identified within the *Ica1* core promoter region are within 1) exon A at (−)471, (−)304, and (−)190; 2) exon B at (−)117; and 3) exon C at (−)70 (Fig. 3).

Functional Impact of NOD Ica1 Promoter Elements on Gene Expression—To determine the functional effects of these SNPs on promoter activity, we first generated a number of reporter gene constructs whereby *Ica1* promoter sequences were fused to the luciferase gene. The functional role of the 5′-flanking region in the regulation of transcription of the *Ica1* gene was assessed by its ability to direct expression of the luciferase gene in a transient transfection assay format using mTEC$^+$ cells, derived from NOD mouse thymus (7), and a mouse B cell line (M12) (17). A 2.6-kb fragment of the C57BL/6 5′-flanking region of the *Ica1* gene was inserted into the luciferase reporter gene pGL3-Basic. This construct exhibited significant luciferase activity when transiently transfected into mTEC$^+$ and M12 cells (Fig. 5, *B* and *C*, respectively). In multiple transfection experiments, the relative expression of luciferase using the pGL3-C57BL/6 promoter expression vector was consistently 10–20-fold greater than the background measured with the pGL3-Basic promoterless vector. Hence, we conclude that the 5′-flanking region of the *Ica1* gene has promoter activity. When using constructs of the corresponding 2.6-kb fragment of the NOD 5′-flanking region of the *Ica1* gene containing the identified SNPs, the reporter activity was markedly reduced in both

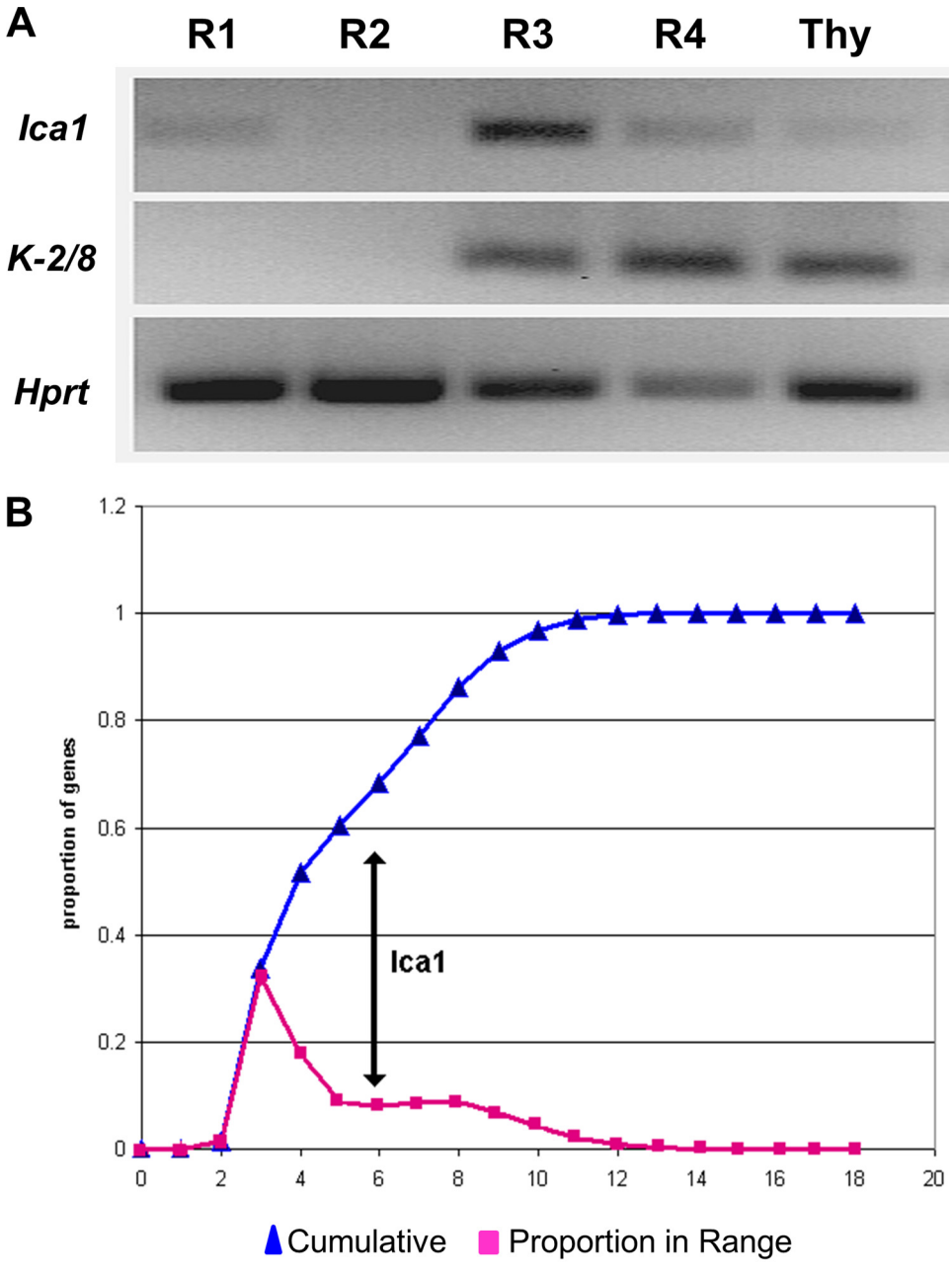

FIGURE 2. *A*, reverse transcriptase PCR analysis of thymic *Ica1* gene expression. Thymi from C57Bl6/129 mice were harvested, digested with collagenase, and separated into four stromal populations via magnetic technology and FACS sorting, as described previously (8). *R1*, $CD45^+$, MHC II^+, $CD11c^-$ macrophages, and B-cells; *R2*, $CD45^+$, MHC II^+, $CD11c^+$ thymic dendritic cells; *R3*, $CD45^-$, $EpCAM^+$, UEA-1^{high}, $Ly51^{low}$ mTECs; *R4*, $CD45^-$, $EpCAM^+$, UEA-1^{low}, $Ly51^{high}$ cortical thymic epithelial cells; *Thy*, whole thymus. *K-2-8*, epithelial cell marker cytokeratin 2/8; *Hprt*, housekeeping gene hypoxanthine-guanine phosphoribosyltransferase as control. As shown, *Ica1* is predominantly expressed in mTECs within the thymus. *B*, expression levels of *Ica1* in the microarray profiling of an insulin-expressing $mTEC^+$ cell line, in relation to a frequency histogram of expression levels of all probes in the microarray. *Ica1* is on the 64th percentile relative to the rest of the transcriptome.

$mTEC^+$ and M12 cells compared with that of the non-diabetic C57BL/6 construct (Fig. 5; $p = 0.01$).

We next investigated the functional significance of the five SNPs identified in the NOD *Ica1* by transient transfection experiments in the $mTEC^+$ and M12 cell lines. Three constructs were generated to analyze different combinations of multiple SNPs from the NOD *Ica1* core promoter when inserted into the wild type promoter backbone of the C57BL/6 (Fig. 5*A*). This analysis revealed that the NOD-specific SNPs were associated with a reduced expression in luciferase activity in both $mTEC^+$ and M12 cells when comparing the mutated C57BL/6 core promoter sequence containing all five NOD SNPs (Construct 3) to the normal C57BL/6 core promoter sequence (Fig. 5, *B* and *C*). The results of the luciferase assays involving four of the five individually mutated SNPs within the NOD putative *Ica1* promoter region did not result in significant changes in transcriptional activity (data not shown).

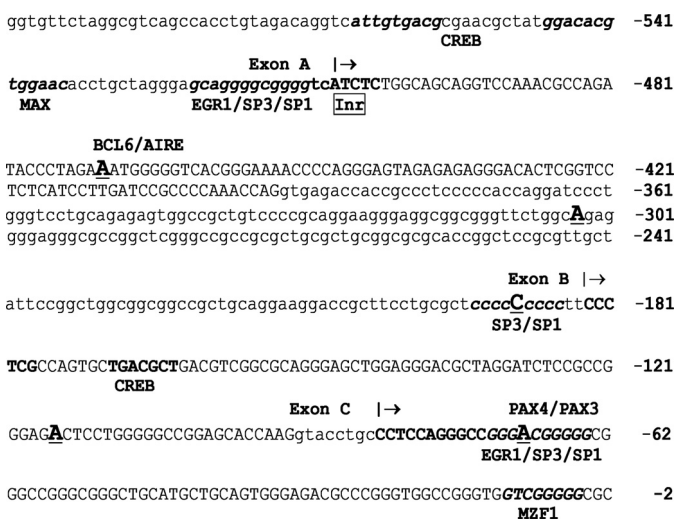

FIGURE 3. **Nucleic acid sequence of the NOD/ShiLtJ strain *Ica1* promoter elements; GenBank™ accession number JF513202.** By alignment analysis and comparison with human *ICA1* promoter sequence, the entire sequence of the mouse putative *Ica1* promoter and flanking regions was confirmed. The nucleotide sequence shows potential transcription activator sequences and binding sites for TFs. Exon sequences are shown in *capital letters*. Intronic sequences are shown in *lowercase letters*, and the consensus initiator (*Inr*) sequence for exon A and exons B and C is illustrated. The five SNPs, (−)471 (C/A), (−)304 (G/A), (−)190 (G/C), (−)117 (G/A), and (−)70 (G/A), within the NOD *Ica1* core promoter sequence are *underlined*.

To further our analysis of the promoter, we performed *in silico* TF binding site analysis and identified several TFs predicted to have allele-specific binding activity at each of the three polymorphic loci in the NOD mouse *Ica1* promoter region (supplemental Table 1). The TFs with the strongest differential binding affinities between alleles are as follows: BCL6 and AIRE at −471 (A/C); E2F1 at −117 (A/G); and PAX4 at −70 (A/G). Many TFs serve as either activators or repressors of gene expression, depending on the cellular context; therefore, the functional consequence of the predicted allele-dependent TF binding affinity was not immediately evident and requires further molecular investigation.

The AIRE transcription factor is highly expressed in the thymus and in extrathymic AIRE-expressing cells (26), wherein it is a critical element in the induction of immunological tolerance (27). To validate the predicted AIRE binding site at position −471 in the NOD *Ica1* promoter, we used the NoShift® assay. Using mTEC$^+$ and M12 nuclear cell extracts, the binding of AIRE to oligonucleotides containing the predicted AIRE binding site (NOD) was stronger relative to oligonucleotides without the AIRE binding site (C57BL/6) (Fig. 6*A*; mTEC$^+$, $p = 0.02$; M12 cells, $p = 0.01$). To support our *in vitro* studies, we provide additional *in vivo* evidence demonstrating that *Ica1* expression of ICA69 is more highly expressed in CD45$^-$ MHC class II$^+$ stromal cells (CD45$^-$, EpCAM$^+$, UEA-1^{high}, Ly51^{low}) isolated from lymph nodes from *Aire*-deficient mice as compared with the same cell subpopulation obtained from C57BL/6 and NOD mice (Fig. 6*B*; $p = 0.001$). Finally, subsequent PCR analysis, using cDNA generated from thymic tissue, showed that expression of ICA69 is significantly reduced in NOD when compared with C57BL/6 (Fig. 6*C*).

DISCUSSION

ICA69, a protein product of human *ICA1* or mouse *Ica1* (12, 18, 28, 29), is predominantly expressed in the islets of Langerhans and neuroendocrine organs (12, 13). This protein and its *Caenorhabditis elegans* homologue, *ric*-19 are conserved regulators of neuroendocrine secretion (30). ICA69 is involved in dense core vesicle signaling and maturation (31) and is recruited to Golgi membranes by activated RAB-2 (32). ICA69 is thought to be a T1D autoantigen based on the following observations: 1) autoantibodies to ICA69 can be detected in both first degree relatives of T1D patients who are followed to overt diabetes and in newly diagnosed diabetic patients (12, 14, 33–35); 2) autoreactive T cells directed to ICA69 can be detected in (*a*) newly diagnosed diabetic children (~80% of patients with recent onset T1D have either ICA69 autoreactive T cells or autoantibodies against the molecule) (29) and (*b*) NOD mice (36, 37); and 3) T cells specific for the murine ICA69 peptide Tep-69 play a driving role in the acceleration of T cell-mediated islet cell destruction in NOD mice, whereas intraperitoneal injection of the peptide Tep-69 is associated with decreased T1D incidence in NOD mice, apparently as a result of neonatal tolerization of unknown mechanism (38). The latter studies are promising and are based on the generation of a NOD mouse T cell hybridoma that recognizes the murine peptide Tep69. Adoptive transfer models of diabetes development were utilized to test the functional significance of the Tep69-specific T cells in NOD mice; intravenous administration of Tep69 peptide into adoptive transfer recipients dramatically accelerated the development of diabetes in NOD mice (36). Moreover, in recombinant congenic strains, which share ~85% of the NOD mouse genome, the presence of CBA/LsLt genome (diabetes-resistant strain) in the region of chromosome 6 where the *Ica1* gene is localized results in mice resistant to both spontaneous insulin-dependent diabetes and cyclophosphamide-induced diabetes (39). More recently, association studies in systemic lupus erythematosus identified *ICA1* as one of the susceptible genetic candidates for this condition, supporting the notion that some common pathways are shared with a number of autoimmune disorders (40, 41).

For the first time, we have characterized the mouse putative *Ica1* promoter elements of C57BL/6 and NOD mouse strains. Our approach to analyzing the *Ica1* 5′-flanking sequences for promoter activity was assisted, in part, by alignment with the human *ICA1* promoter and by computer analysis of the flanking sequences for potential transcription activator sequences and TF binding sites. There is a high degree of identity between the mouse *Ica1* and human *ICA1* core promoters (18). We further show that the *Ica1* promoter region is polymorphic (namely there are five SNPs distinguishing the NOD from the C57BL/6 sequence) and that the NOD-derived *Ica1* promoter exhibits markedly reduced reporter activity in both mTEC$^+$ and M12 cells compared with the C57BL/6-derived promoter. Although mutagenesis of the C57BL/6-derived promoter at four of five individual SNP loci did not reduce reporter activity, the insertion of multiple SNPs did, suggesting that the SNPs may have a combined effect.

Despite the paucity of data on the mechanism of ICA69-based tolerance induction in NOD neonatal mice, our results support the existence of more fundamental means of autoreac-

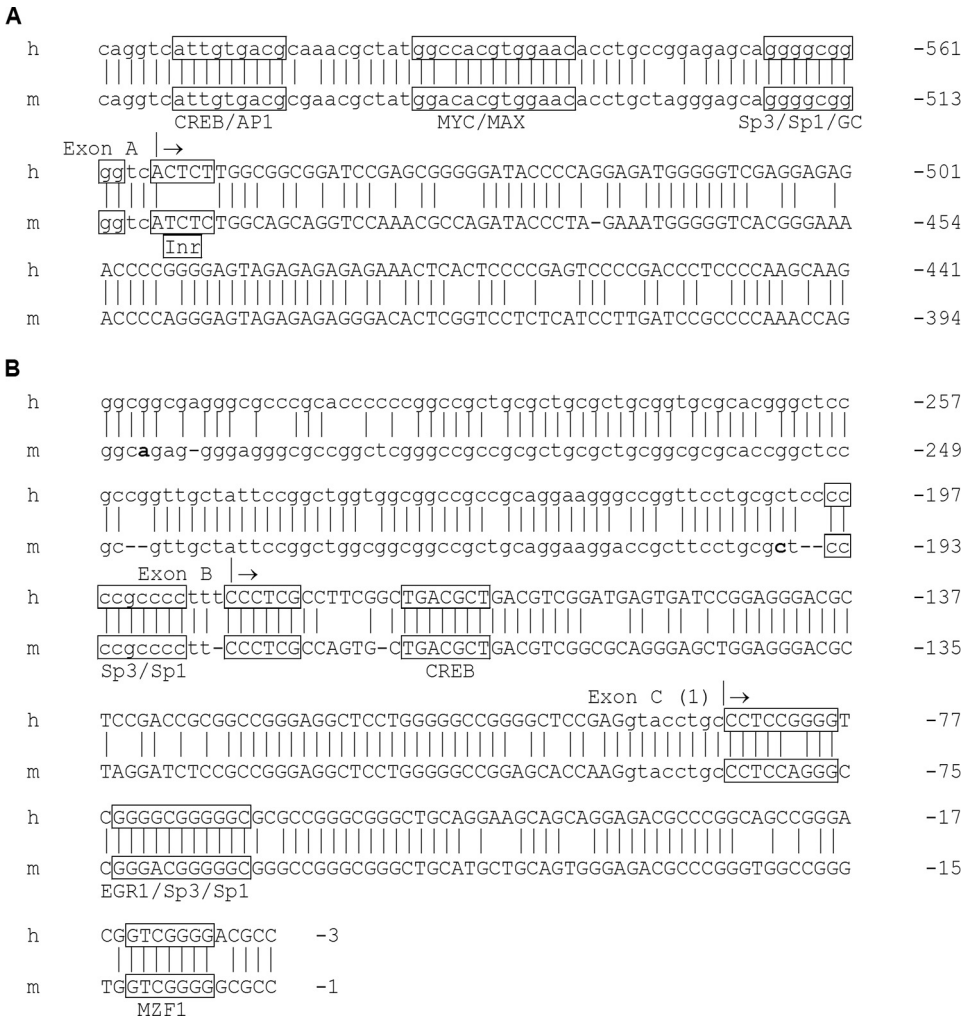

FIGURE 4. **Significant sequence identity is shared between the NOD mouse *Ica1* promoter and the human *ICA1* promoter.** The alignment of major elements, including exons A, B, and C along with the intron sequences in close proximity of the NOD mouse *Ica1* and human *ICA1* promoters, shows considerable identity. *A*, exon A and the close flanking intron sequence show 79% identity between humans (*h*) and mice (*m*). In addition, the potential transcription activator sequences and TF binding sites show an even higher sequence identity. *B*, both exons B and C show 82% sequence identity between humans and mice. Remarkably, the sequence identity in the potential transcription activator sequences and TF binding sites is 100%.

tivity control based on the expression of this putative autoantigen in the thymus, whereby *Ica1* transcription levels may be under the direct effects of promoter sequence variants. Our previous findings indicated that thymic expression of ICA69 is reduced in NOD as compared with a number of control mice (15). Although these experiments do not provide definitive evidence to a precise molecular mechanism to account for this observation, they do imply that either the polymorphic *Ica1* NOD promoter, or a haplotype in linkage disequilibrium with it, may modulate *Ica1* promoter activity of the thymus which is believed to be intrinsic to T1D susceptibility. The resulting reduction in thymic expression of ICA69 in the NOD mouse might contribute to the loss of immunologic tolerance in this model of autoimmune diabetes.

Genetic variations resulting in defective thymic expression of islet cell autoantigens have been implicated in the loss of immunologic tolerance to these autoantigens. Functional variation of *INS* promoter conferred by the VNTR polymorphism has been associated with reduced insulin expression in the thymus and in lymphoid organs (42, 43). Another example is provided by the autoimmune polyendocrine syndrome type I, which is a monogenic disease caused by mutations within the AIRE locus (44). Of note, AIRE-deficient mice develop a multiorgan autoimmunity characterized by lymphocytic infiltrates and autoantibodies, resembling those abnormalities seen in autoimmune polyendocrine syndrome type I, along with a specific reduction in ectopic transcription of genes encoding peripheral self-antigens (45, 46). In the present study, we demonstrate that a newly identified polymorphic *Ica1* promoter may account for reduced expression of ICA69 in the thymus of NOD mice, which may play a role in T1D susceptibility.

Interestingly, luciferase reporter constructs demonstrated that the C57BL/6 *Ica1* promoter region was transcriptionally active not only in $mTEC^{+}$ but also in M12 B-cell-derived cell lines (17). B cell antigen capture and presentation, associated with determinant antigen spreading, has become a very popular concept since the previously reported results of the rituximab treatment in NOD mice and in human T1D showing delay in disease progression as a result of transient B cell depletion (47–49).

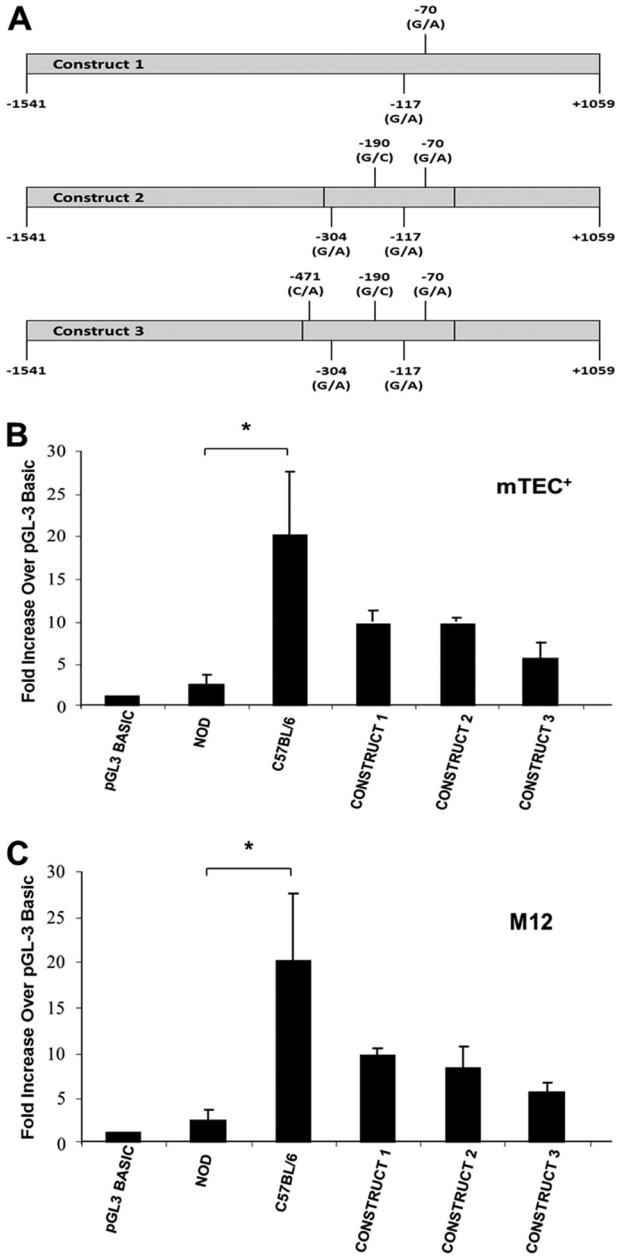

FIGURE 5. *A*, schematic representation of three constructs with mutations within the *Ica1* core promoter that were utilized in luciferase assays. Different combinations of SNPs from the *Ica1* promoter NOD strain were inserted into the wild type promoter backbone (C57BL/6). *B*, mTEC$^+$ cells were transiently transfected with putative *Ica1* promoter element constructs or pGL3-Basic reporter vector positive and negative controls. The transcriptional activity driven by the putative Ica1 promoter element inserted within its promoter site of pGL3-Basic reporter vector was assessed by luciferase activity. The luciferase assay showed an approximately 8-fold reduction of enzyme and transcription activity from the NOD *Ica1* putative promoter element as compared with the C57BL/6 putative *Ica1* promoter (*, $p = 0.01$). Mutated SNPs found in the NOD promoter element also illustrate reduced enzyme and transcriptional activity. Results are expressed as mean ± S.E. (*error bars*) of 5–7 independent sets of transfection experiments performed in triplicate. *C*, M12 cells were transiently transfected with putative Ica1 promoter element constructs or pGL3-Basic reporter vector positive and negative controls. The transcriptional activity driven by the putative *Ica1* promoter element inserted within the promoter site for the pGL3 reporter was assessed by luciferase. The luciferase assay shows a 20-fold reduction of enzyme and transcription activity for the NOD *Ica1* putative promoter element as compared with the C57BL/6 putative *Ica1* promoter (*, $p = 0.01$). Mutated SNPs found in the NOD promoter element also showed reduced enzyme and transcriptional activity. Results are expressed as mean ± S.E. of 5–7 independent sets of transfection experiments performed in triplicate.

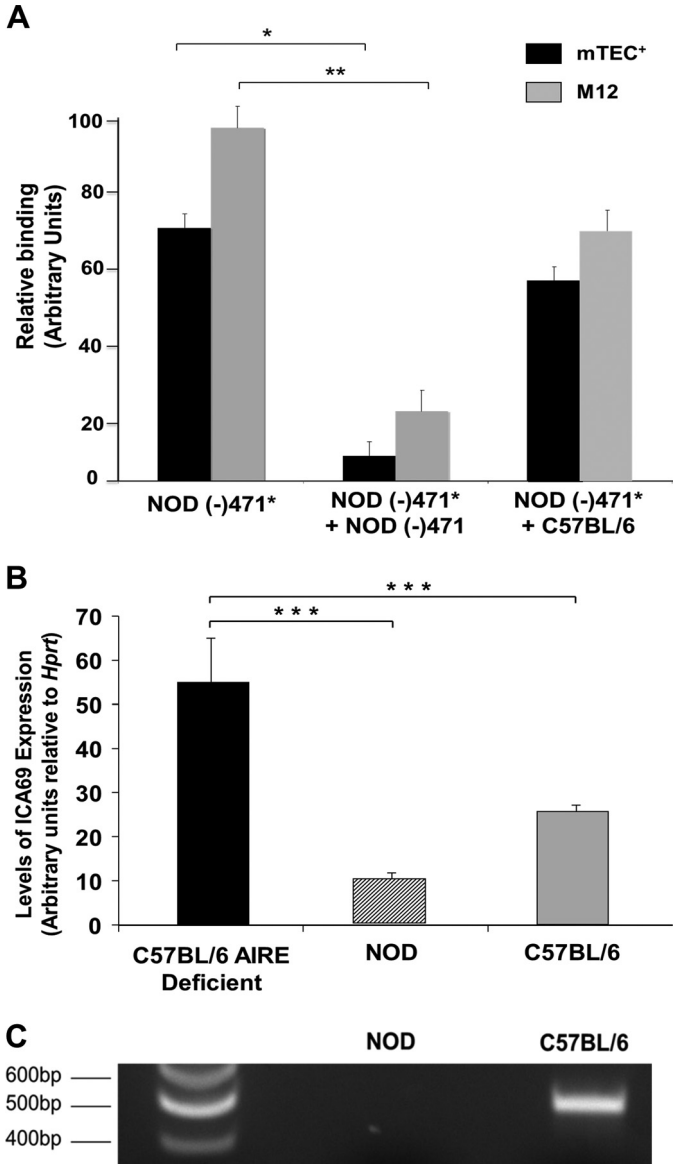

FIGURE 6. **AIRE TF binding to the NOD *Ica1* core promoter and *Ica1* expression.** *A*, nuclear extracts containing the AIRE TF were incubated with double-stranded oligonucleotides (Table 1) to determine the AIRE binding specificity for the NOD SNP at base pair (−)471 of the *Ica1* promoter. Binding to oligonucleotides containing the NOD single AIRE TF binding site was substantially greater than that of the C57BL/6 oligonucleotide (lacking the AIRE TF binding site) with nuclear proteins from both mTEC$^+$ (*, $p = 0.02$) and M12 cells (**, $p = 0.01$). Specificity for the NOD (−)471 SNP is shown in columns whereby the non-biotinylated C57BL/6 oligonucleotide does not compete out for the biotinylated NOD (−)471 oligonucleotide, whereas the non-biotinylated NOD (−)471 does compete. The data are reported as the mean ± S.E. of three independent triplicates. *B*, high ICA69 expression in lymph node stromal cells of AIRE-deficient mice. CD45$^-$ MHC II$^+$ lymphoid stromal cells were isolated from NOD, C57BL/6, and AIRE-deficient mice (B6.129S2-*Aire*$^{tm1.1Doi}$/J) and were subjected to quantitative RT-PCR analysis of ICA69 expression. Data are presented as arbitrary units relative to *hprt* controls (mean ± S.E. (*error bars*), $n = 3$ C57BL/6 and $n = 3$ AIRE-deficient mice; ***, $p < 0.001$). *C*, amplification of a 500-base pair fragment of *Ica1* from cDNA generated from C57BL/6 thymic tissue. A 500-bp specific band is present only for the C57BL/6. This PCR fragment was gel-purified, and nucleotide sequence was verified.

Our study predicts several TFs that have allele-specific binding at each of three mutant loci in the *Ica1* promoter region. It is possible that the loss/gain of one or more of these TF binding events

may contribute to the observed differences in the activity of the mutant *Ica1* promoter. Encouragingly, a number of the TFs identified are key regulators of processes relevant to *Ica1* gene function and autoimmunity (*e.g.* BCL6 (50) and AIRE (51)).

The TF AIRE controls the expression of a set of tissue-specific antigens in medullary thymic epithelial cells whereby self-reactive T cells undergo negative selection (52, 53). Autoimmune disease ensuing from a loss of self-tolerance is clinically and genetically complex and has many potential etiological causes. Evidence indicates that it is commonly linked to defects in the thymic epithelial and lymphoid microenvironment.

We found that that ICA69 is more highly expressed in stromal cells ($CD45^-$ MHC class II^+) isolated from lymph nodes from AIRE-deficient mice as compared with the same cell subpopulation obtained from B6 mice. Hence, our findings suggest that AIRE may be directly involved in controlling the expression of ICA69 in $mTEC^+$ and in extrathymic AIRE-expressing cells. Furthermore, our results provide experimental evidence for preferential binding of AIRE to the NOD mouse *Ica1* promoter, where it functions as a transcriptional repressor, thereby down-regulating ICA69 expression.

Previous analyses of gene expression patterns in AIRE-deficient mice indicate that AIRE may function as either a transcriptional activator or a repressor, depending on the promoter context (51, 54). It has been found that AIRE can act as a transcriptional repressor on the promoter of the housekeeping gene encoding cystatin B (51). The effects of AIRE on different gene promoters are modulated by interactions with other transcriptional regulators, such as PIAS1, but might also depend on DNA elements or the chromatin structure of the specific promoter (51, 55).

In summary, this is the first report describing the mouse *Ica1* core promoter DNA sequence providing evidence that SNPs within this region are unique and functionally distinguishable between the diabetes-prone NOD mouse and the control C57BL/6 mouse strain. These SNPs provide potential functional relevance to the development of autoimmunity, which may translate into similar effects in human disease. This variation may be functionally linked to reduced thymic expression of ICA69 secondary to AIRE-mediated down-regulation of ICA69 expression and be directly involved in thymus-specific processes of negative selection of ICA69-reactive developing thymocytes. Altogether, *Ica1* may be an additional gene involved in the maintenance of central tolerance to β cell-restricted antigens, and deciphering its expression mechanisms *in vivo* will lead to a more comprehensive understanding of the role of the thymus and other lymphoid organs in islet autoimmunity.

Acknowledgments—We thank Dr. W. Dunnick for providing the M12 cells and Drs. R. Menon and T. Smith for helpful discussions. We also thank D. Stenger for critical reading of the manuscript. Tissues were provided by Drs. C. K. Petito and I. Logvisnki (Diabetes Research Institute Cell Transplant Center Team, University of Miami Brain and Fetal Tissue Bank; a joint effort with the University of Maryland Brain and Tissue Banks through National Institutes of Health, NICHD, Contract NO1-HD-8-3284).

REFERENCES

1. Jolicoeur, C., Hanahan, D., and Smith, K. M. (1994) T-cell tolerance toward a transgenic β-cell antigen and transcription of endogenous pancreatic genes in thymus. *Proc. Natl. Acad. Sci. U.S.A.* **91,** 6707–67011
2. Pugliese, A., Zeller, M., Fernandez, A., Jr., Zalcberg, L. J., Bartlett, R. J., Ricordi, C., Pietropaolo, M., Eisenbarth, G. S., Bennett, S. T., and Patel, D. D. (1997) The insulin gene is transcribed in the human thymus and transcription levels correlated with allelic variation at the INS VNTR-IDDM2 susceptibility locus for type 1 diabetes. *Nat. Genet.* **15,** 293–297
3. Nitta, T., Murata, S., Ueno, T., Tanaka, K., and Takahama, Y. (2008) Thymic microenvironments for T-cell repertoire formation. *Adv. Immunol.* **99,** 59–94
4. Hanahan, D. (1998) Peripheral antigen-expressing cells in thymic medulla. Factors in self-tolerance and autoimmunity. *Curr. Opin. Immunol.* **10,** 656–662
5. DeVoss, J. J., and Anderson, M. S. (2007) Lessons on immune tolerance from the monogenic disease APS1. *Curr. Opin. Genet. Dev.* **17,** 193–200
6. Nakayama, M., Abiru, N., Moriyama, H., Babaya, N., Liu, E., Miao, D., Yu, L., Wegmann, D. R., Hutton, J. C., Elliott, J. F., and Eisenbarth, G. S. (2005) Prime role for an insulin epitope in the development of type 1 diabetes in NOD mice. *Nature* **435,** 220–223
7. Palumbo, M. O., Levi, D., Chentoufi, A. A., and Polychronakos, C. (2006) Isolation and characterization of proinsulin-producing medullary thymic epithelial cell clones. *Diabetes* **55,** 2595–2601
8. Fan, Y., Rudert, W. A., Grupillo, M., He, J., Sisino, G., and Trucco, M. (2009) Thymus-specific deletion of insulin induces autoimmune diabetes. *EMBO J.* **28,** 2812–2824
9. Sabater, L., Ferrer-Francesch, X., Sospedra, M., Caro, P., Juan, M., and Pujol-Borrell, R. (2005) Insulin alleles and autoimmune regulator (AIRE) gene expression both influence insulin expression in the thymus. *J. Autoimmun.* **25,** 312–318
10. Vafiadis, P., Bennett, S. T., Todd, J. A., Nadeau, J., Grabs, R., Goodyer, C. G., Wickramasinghe, S., Colle, E., and Polychronakos, C. (1997) Insulin expression in human thymus is modulated by INS VNTR alleles at the IDDM2 locus. *Nat. Genet.* **15,** 289–292
11. Vafiadis, P., Bennett, S. T., Todd, J. A., Grabs, R., and Polychronakos, C. (1998) Divergence between genetic determinants of IGF2 transcription levels in leukocytes and of IDDM2-encoded susceptibility to type 1 diabetes. *J. Clin. Endocrinol. Metab.* **83,** 2933–2939
12. Pietropaolo, M., Castaño, L., Babu, S., Buelow, R., Kuo, Y. L., Martin, S., Martin, A., Powers, A. C., Prochazka, M., Naggert, J., Leiter, E. H., and Eisenbarth, G. S. (1993) Islet cell autoantigen 69 kD (ICA69). Molecular cloning and characterization of a novel diabetes-associated autoantigen. *J. Clin. Invest.* **92,** 359–371
13. Karges, W., Pietropaolo, M., Ackerley, C. A., and Dosch, H. M. (1996) Gene expression of islet cell antigen p69 in human, mouse, and rat. *Diabetes* **45,** 513–521
14. Song, A., Winer, S., Tsui, H., Sampson, A., Pasceri, P., Ellis, J., Elliott, J. F., and Dosch, H. M. (2003) Deviation of islet autoreactivity to cryptic epitopes protects NOD mice from diabetes. *Eur. J. Immunol.* **33,** 546–555
15. Mathews, C. E., Pietropaolo, S. L., and Pietropaolo, M. (2003) Reduced thymic expression of islet antigen contributes to loss of self-tolerance. *Ann. N.Y. Acad. Sci.* **1005,** 412–417
16. Dogra, R. S., Vaidyanathan, P., Prabakar, K. R., Marshall, K. E., Hutton, J. C., and Pugliese, A. (2006) Alternative splicing of G6PC2, the gene coding for the islet-specific glucose-6-phosphatase catalytic subunit-related protein (IGRP), results in differential expression in human thymus and spleen compared with pancreas. *Diabetologia* **49,** 953–957
17. Glimcher, L. H., Hamano, T., Asofsky, R., Herber-Katz, E., Hedrick, S., Schwartz, R. H., and Paul, W. E. (1982) I region-restricted antigen presentation by B cell-B lymphoma hybridomas. *Nature* **298,** 283–284
18. Friday, R. P., Pietropaolo, S. L., Profozich, J., Trucco, M., and Pietropaolo, M. (2003) Alternative core promoters regulate tissue-specific transcription from the autoimmune diabetes-related ICA1 (ICA69) gene locus.

J. Biol. Chem. **278,** 853–863
19. Hannenhalli, S., and Levy, S. (2003) Transcriptional regulation of protein complexes and biological pathways. *Mamm. Genome* **14,** 611–619
20. Bruggink, F., and Hayes, S. (2004) Identification of DNA binding proteins using the NoShift transcription factor assay kit. *Nat. Methods* **1,** 177–179
21. Pugliese, A., Brown, D., Garza, D., Murchison, D., Zeller, M., Redondo, M. J., Diez, J., Eisenbarth, G. S., Patel, D. D., and Ricordi, C. (2001) Self-antigen-presenting cells expressing diabetes-associated autoantigens exist in both thymus and peripheral lymphoid organs. *J. Clin. Invest.* **107,** 555–564
22. Schmid, I., Uittenbogaart, C. H., and Giorgi, J. V. (1991) A gentle fixation and permeabilization method for combined cell surface and intracellular staining with improved precision in DNA quantification. *Cytometry* **12,** 279–285
23. Fletcher, A. L., Calder, A., Hince, M. N., Boyd, R. L., and Chidgey, A. P. (2011) The contribution of thymic stromal abnormalities to autoimmune disease. *Crit. Rev. Immunol.* **31,** 171–187
24. Hubert, F. X., Kinkel, S. A., Webster, K. E., Cannon, P., Crewther, P. E., Proeitto, A. I., Wu, L., Heath, W. R., and Scott, H. S. (2008) A specific anti-Aire antibody reveals aire expression is restricted to medullary thymic epithelial cells and not expressed in periphery. *J. Immunol.* **180,** 3824–3832
25. Gaedigk, R., Duncan, A. M., Miyazaki, I., Robinson, B. H., and Dosch, H. M. (1994) ICA1 encoding p69, a protein linked to the development of type 1 diabetes, maps to human chromosome 7p22. *Cytogenet. Cell Genet.* **66,** 274–276
26. Gardner, J. M., Devoss, J. J., Friedman, R. S., Wong, D. J., Tan, Y. X., Zhou, X., Johannes, K. P., Su, M. A., Chang, H. Y., Krummel, M. F., and Anderson, M. S. (2008) Deletional tolerance mediated by extrathymic Aire-expressing cells. *Science* **321,** 843–847
27. Kyewski, B., and Peterson, P. (2010) Aire, master of many trades. *Cell* **140,** 24–26
28. Spitzenberger, F., Pietropaolo, S., Verkade, P., Habermann, B., Lacas-Gervais, S., Mziaut, H., Pietropaolo, M., and Solimena, M. (2003) Islet cell autoantigen of 69 kDa is an arfaptin-related protein associated with the Golgi complex of insulinoma INS-1 cells. *J. Biol. Chem.* **278,** 26166–26173
29. Gaedigk, R., Karges, W., Hui, M. F., Scherer, S. W., and Dosch, H. M. (1996) Genomic organization and transcript analysis of ICAp69, a target antigen in diabetic autoimmunity. *Genomics* **38,** 382–391
30. Pilon, M., Peng, X. R., Spence, A. M., Plasterk, R. H., and Dosch, H. M. (2000) The diabetes autoantigen ICA69 and its *Caenorhabditis elegans* homologue, RIC-19, are conserved regulators of neuroendocrine secretion. *Mol. Biol. Cell* **11,** 3277–3288
31. Sumakovic, M., Hegermann, J., Luo, L., Husson, S. J., Schwarze, K., Olendrowitz, C., Schoofs, L., Richmond, J., and Eimer, S. (2009) UNC-108/RAB-2 and its effector RIC-19 are involved in dense core vesicle maturation in Caenorhabditis elegans. *J. Cell Biol.* **186,** 897–914
32. Buffa, L., Fuchs, E., Pietropaolo, M., Barr, F., and Solimena, M. (2008) ICA69 is a novel Rab2 effector regulating ER-Golgi trafficking in insulinoma cells. *Eur. J. Cell Biol.* **87,** 197–209
33. Martin, S., Kardorf, J., Schulte, B., Lampeter, E. F., Gries, F. A., Melchers, I., Wagner, R., Bertrams, J., Roep, B. O., and Pfützner, A. (1995) Autoantibodies to the islet antigen ICA69 occur in IDDM and in rheumatoid arthritis. *Diabetologia* **38,** 351–355
34. Roep, B. O., Duinkerken, G., Schreuder, G. M., Kolb, H., de Vries, R. R., and Martin, S. (1996) HLA-associated inverse correlation between T cell and antibody responsiveness to islet autoantigen in recent-onset insulin-dependent diabetes mellitus. *Eur. J. Immunol.* **26,** 1285–1289
35. Dosch, H., Cheung, R. K., Karges, W., Pietropaolo, M., and Becker, D. J. (1999) Persistent T cell anergy in human type 1 diabetes. *J. Immunol.* **163,** 6933–6940
36. Winer, S., Gunaratnam, L., Astsatourov, I., Cheung, R. K., Kubiak, V., Karges, W., Hammond-McKibben, D., Gaedigk, R., Graziano, D., Trucco, M., Becker, D. J., and Dosch, H. M. (2000) Peptide dose, MHC affinity, and target self-antigen expression are critical for effective immunotherapy of nonobese diabetic mouse prediabetes. *J. Immunol.* **165,** 4086–4094
37. Chen, W., Bergerot, I., Elliott, J. F., Harrison, L. C., Abiru, N., Eisenbarth, G. S., and Delovitch, T. L. (2001) Evidence that a peptide spanning the B-C junction of proinsulin is an early autoantigen epitope in the pathogenesis of type 1 diabetes. *J. Immunol.* **167,** 4926–4935
38. Karges, W., Hammond-McKibben, D., Gaedigk, R., Shibuya, N., Cheung, R., and Dosch, H. M. (1997) Loss of self-tolerance to ICA69 in nonobese diabetic mice. *Diabetes* **46,** 1548–1556
39. Reifsnyder, P. C., Flynn, J. C., Gavin, A. L., Simone, E. A., Sharp, J. J., Herberg, L., and Leiter, E. H. (1999) Genotypic and phenotypic characterization of six new recombinant congenic strains derived from NOD/Shi and CBA/J genomes. *Mamm. Genome* **10,** 161–167
40. International Consortium for Systemic Lupus Erythematosus Genetics (SLEGEN), Harley, J. B., Alarcón-Riquelme, M. E., Criswell, L. A., Jacob, C. O., Kimberly, R. P., Moser, K. L., Tsao, B. P., Vyse, T. J., Langefeld, C. D., Nath, S. K., Guthridge, J. M., Cobb, B. L., Mirel, D. B., Marion, M. C., Williams, A. H., Divers, J., Wang, W., Frank, S. G., Namjou, B., Gabriel, S. B., Lee, A. T., Gregersen, P. K., Behrens, T. W., Taylor, K. E., Fernando, M., Zidovetzki, R., Gaffney, P. M., Edberg, J. C., Rioux, J. D., Ojwang, J. O., James, J. A., Merrill, J. T., Gilkeson, G. S., Seldin, M. F., Yin, H., Baechler, E. C., Li, Q. Z., Wakeland, E. K., Bruner, G. R., Kaufman, K. M., and Kelly, J. A. (2008) Genome-wide association scan in women with systemic lupus erythematosus identifies susceptibility variants in ITGAM, PXK, KIAA1542 and other loci. *Nat. Genet.* **40,** 204–210
41. Budarf, M. L., Goyette, P., Boucher, G., Lian, J., Graham, R. R., Claudio, J. O., Hudson, T., Gladman, D., Clarke, A. E., Pope, J. E., Peschken, C., Smith, C. D., Hanly, J., Rich, E., Boire, G., Barr, S. G., Zummer, M., GenES Investigators, Fortin, P. R., Wither, J., and Rioux, J. D. (2011) A targeted association study in systemic lupus erythematosus identifies multiple susceptibility alleles. *Genes Immun.* **12,** 51–58
42. Vafiadis, P., Ounissi-Benkalha, H., Palumbo, M., Grabs, R., Rousseau, M., Goodyer, C. G., and Polychronakos, C. (2001) Class III alleles of the variable number of tandem repeat insulin polymorphism associated with silencing of thymic insulin predispose to type 1 diabetes. *J. Clin. Endocrinol. Metab.* **86,** 3705–3710
43. Durinovic-Belló, I., Jelinek, E., Schlosser, M., Eiermann, T., Boehm, B. O., Karges, W., Marchand, L., and Polychronakos, C. (2005) Class III alleles at the insulin VNTR polymorphism are associated with regulatory T-cell responses to proinsulin epitopes in HLA-DR4, DQ8 individuals. *Diabetes* **54,** S18-S24
44. Nagamine, K., Peterson, P., Scott, H. S., Kudoh, J., Minoshima, S., Heino, M., Krohn, K. J., Lalioti, M. D., Mullis, P. E., Antonarakis, S. E., Kawasaki, K., Asakawa, S., Ito, F., and Shimizu, N. (1997) Positional cloning of the APECED gene. *Nature Genet.* **17,** 393–398
45. Anderson, M. S., Venanzi, E. S., Klein, L., Chen, Z., Berzins, S. P., Turley, S. J., von Boehmer, H., Bronson, R., Dierich, A., Benoist, C., and Mathis, D. (2002) Projection of an immunological self shadow within the thymus by the aire protein. *Science* **298,** 1395–1401
46. Ramsey, C., Winqvist, O., Puhakka, L., Halonen, M., Moro, A., Kämpe, O., Eskelin, P., Pelto-Huikko, M., and Peltonen, L. (2002) Aire-deficient mice develop multiple features of APECED phenotype and show altered immune response. *Hum. Mol. Genet.* **11,** 397–409
47. Xiu, Y., Wong, C. P., Bouaziz, J. D., Hamaguchi, Y., Wang, Y., Pop, S. M., Tisch, R. M., and Tedder, T. F. (2008) B lymphocyte depletion by CD20 monoclonal antibody prevents diabetes in nonobese diabetic mice despite isotype-specific differences in FcγR effector functions. *J. Immunol.* **180,** 2863–2875
48. Pescovitz, M. D., Greenbaum, C. J., Krause-Steinrauf, H., Becker, D. J., Gitelman, S. E., Goland, R., Gottlieb, P. A., Marks, J. B., McGee, P. F., Moran, A. M., Raskin, P., Rodriguez, H., Schatz, D. A., Wherrett, D., Wilson, D. M., Lachin, J. M., and Skyler, J. S. (2009) Rituximab, B-lymphocyte depletion, and preservation of β-cell function. *N. Engl. J. Med.* **361,** 2143–2152
49. O'Neill, S. K., Liu, E., and Cambier, J. C. (2009) Change you can B(cell)eive in. Recent progress confirms a critical role for B cells in type 1 diabetes. *Curr. Opin. Endocrinol. Diabetes Obes.* **16,** 293–298
50. Igoillo-Esteve, M., Gurzov, E. N., Eizirik, D. L., and Cnop, M. (2011) The transcription factor B-cell lymphoma (BCL)-6 modulates pancreatic

β-cell inflammatory responses. *Endocrinology* **152,** 447–456
51. Peterson, P., Org, T., and Rebane, A. (2008) Transcriptional regulation by AIRE. Molecular mechanisms of central tolerance. *Nat. Rev. Immunol.* **8,** 948–957
52. Mathis, D., and Benoist, C. (2009) Aire. *Annu. Rev. Immunol.* **27,** 287–312
53. Anderson, M. S., and Su, M. A. (2011) Aire and T cell development. *Curr. Opin. Immunol.* **23,** 198–206
54. Kumar, P. G., Laloraya, M., Wang, C. Y., Ruan, Q. G., Davoodi-Semiromi, A., Kao, K. J., and She, J. X. (2001) The autoimmune regulator (AIRE) is a DNA-binding protein. *J. Biol. Chem.* **276,** 41357–41364
55. Abramson, J., Giraud, M., Benoist, C., and Mathis, D. (2010) Aire's partners in the molecular control of immunological tolerance. *Cell* **140,** 123–135